

Cl chemisorption on the Ag(001) surface: Geometry and electronic structure

H. S. Greenside

Department of Physics, Princeton University, Princeton, New Jersey 08544

D. R. Hamann

Bell Laboratories, Murray Hill, New Jersey 07974

(Received 24 October 1980)

Simple overlayer and mixed-layer geometries are studied for the observed $c(2 \times 2)$ structure of atomic Cl adsorbed on the Ag(001) surface. A self-consistent, Gaussian, linear-combination-of-atomic-orbitals technique with a local exchange-correlation potential is used. Reference calculations are performed for bulk Ag, the clean Ag(001) surface, and an isolated $c(2 \times 2)$ Cl layer. The calculated total and partial density of states for the two geometries are compared with angle-integrated and angle-resolved photoemission experiments. The mixed-layer model gives close agreement with experiment while the overlayer model predicts a single Cl feature above the Ag d band, contrary to the photoemission data. Discrepancies between these calculations and a low-energy electron diffraction study of this system are discussed.

I. INTRODUCTION

Two important steps toward understanding surface phenomena such as epitaxial growth, oxidation, surface diffusion, and heterogeneous catalysis are, first, to obtain detailed information about the geometrical position of adatoms on metal surfaces and, second, to understand how a particular adatom site affects the electronic structure of the adatom bond.

Self-consistent calculations of the electronic structure of adlayers are crucial in utilizing experimental data fully to achieve these two steps.¹ Low-energy electron diffraction (LEED) directly gives the superstructure order, but depends on a detailed analysis to choose a most probable atomic configuration and set of geometric parameters. Angle-resolved ultraviolet photoemission spectroscopy (ARUPS) offers a wealth of detailed information about electronic structure but gives no direct geometrical information.² A self-consistent calculation, based on the geometry derived from a LEED study, is capable of making accurate and specific predictions about bond strength, bond ionicity, work function, orbital content (e.g., the degree to which d , rather than s or p , orbitals from the Ag surface contribute to the bonding), band structure, and density of states (DOS). The latter two may be compared directly with ARUPS data. The dependence of these predictions on an assumed geometry provides an independent approach to geometry determinations and offers new information on the nature of the adatom bond.

In this paper we use a self-consistent, Gaussian, linear-combination-of-atomic-orbitals (LCAO) technique with a local exchange-correlation potential to study the $c(2 \times 2)$ Cl layer on the Ag(001)

surface. The only physical, as opposed to numerical, approximations are the use of a three-layer metal slab to model the semi-infinite Ag solid and the Wigner interpolation formula for the local exchange-correlation potential.³ The thickness of the slab limits the extent to which details of the electronic spectrum can be resolved, but this will be seen to be unimportant for the principal conclusions reached. The only input needed is the geometrical positions of the Cl and Ag atoms in the unit cell of the slab. The results are parameter free. The calculated DOS may be compared directly with features in the photoemission intensity which are independent of photon energy. Final-state and matrix-element effects may be ignored for these features, and the intensity depends primarily on the density of initial states.^{1,2}

A recent LEED study of the $c(2 \times 2)$ Cl on Ag(001) system⁴ examines two likely arrangements of the adatoms in the C_4 symmetry sites of the (001) surface. One arrangement is a mixed-layer model (MLM) in which the Cl adatoms are roughly coplanar with the surface [see Fig. 1(b)]. The other possibility is a simple overlayer model (SOM) in which the Cl atoms sit above the Ag surface [Fig. 1(a)]. The $c(2 \times 2)$ Cl on Ag(001) system is a good system to test the geometry dependence of a self-consistent calculation with the available photoemission data. As we shall see, the MLM yields a DOS in close agreement with the photoemission data while the SOM yields a single Cl-derived peak lying above the Ag d -band emission intensity, contrary to the data. The LEED analysis favors the SOM, however, and we are faced with a serious contradiction which must be resolved by future research.

The rest of the paper has four sections. In Sec.

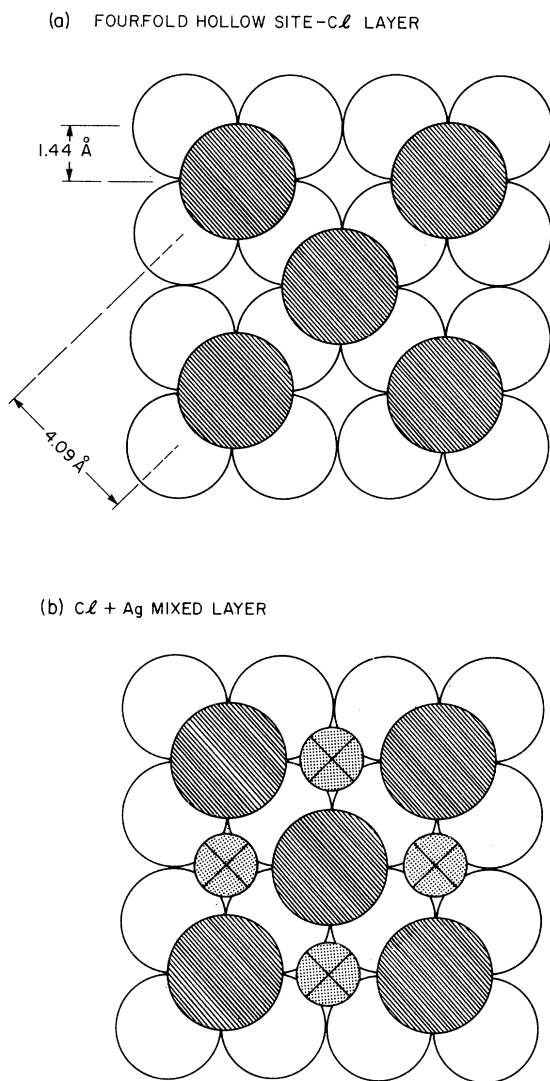


FIG. 1. Schematic picture of the two $c(2 \times 2)$ superstructures of Cl on the Ag(001) surface studied in this paper. (a) Simple overlayer model (SOM). (b) Mixed-layer model (MLM). Open circles, black circles, and hatched circles are substrate Ag atoms, Cl adatoms, and Ag adatoms, respectively.

II we summarize the experimental information obtained by LEED and photoemission spectroscopy. In Sec. III we briefly review the method of calculation and discuss several approximations used. In Sec. IV we present the results and compare them with experiment. We summarize our conclusions in Sec. V.

II. EXPERIMENTAL DATA

The positions of the Cl adatoms were determined by an LEED analysis in which four dif-

ferent geometric models were tested.⁴ The two $c(2 \times 2)$ models considered besides the MLM and SOM were an atop model (AM), in which the adatom lies directly above a surface Ag atom, and a bridge-site model (BM), in which the adatom lies above and between the two adjacent surface Ag atoms. In all four cases, the distance from the adatoms to the surface plane was varied in small increments in order to match calculated LEED intensity curves with the actual data. The LEED data ruled out the AM and BM for all reasonable surface distances while the SOM and MLM, which both gave agreement of roughly the same quality for many beams, were distinguished only if the full set of 21 beams at three polar angles and one angle of azimuth was used. Optimal agreement with most beams was found between the calculated and measured LEED intensities if, in the SOM, the Cl adatoms sat about 1.72 Å above the Ag surface. For the best agreement that could be achieved in the MLM, the Ag surface relaxed in toward the substrate by about 0.1 Å and the Cl adatoms lay in a plane about 0.24 Å closer to the substrate than the Ag surface atoms. The SOM gave better agreement for most beams.

The electronic structure of the $c(2 \times 2)$ Cl adlayer on the Ag(001) surface was probed by angle-integrated and angle-resolved photoemission experiments.⁵ In Figs. 2 and 3 we present some of the photoemission data (which we later compare with our calculated DOS). In Fig. 2 we see angle-integrated energy distribution curves (EDC's) at several different exposures to chlorine gas. The two peaks in the EDC for the clean Ag(001) surface at -4.5 and -6.5 eV are d -band features due to normally oriented (d_{z^2} -like) and oriented closer to parallel (d_{xy} , d_{xz} , d_{yz} -like) d bands, respectively.⁶ As the clean surface is exposed to Cl gas, the emission from the Ag $5sp$ bands (between 0 and -3 eV) becomes attenuated, the d -band feature at -4.5 eV broadens, and the lower feature at -6.5 eV is masked. More detail is obtained by subtracting the clean surface EDC from the other three curves (Fig. 3). Again we see the attenuation of the $5sp$ -band emission, but now we see two features at -3.5 and -6 eV which grow with increasing exposure. These may be associated with emission from the Cl adatom orbitals.⁵ The increasing attenuation of the d -band emission between -4 and -5.5 eV together with the increasing emission from the Cl orbitals as exposure increases suggests that the Ag $4d$ bands are involved in the adatom bonding.

Angle-resolved photoemission data from this same study⁶ give the dispersion of the various features as a function of \vec{k}_{\parallel} , the electron mo-

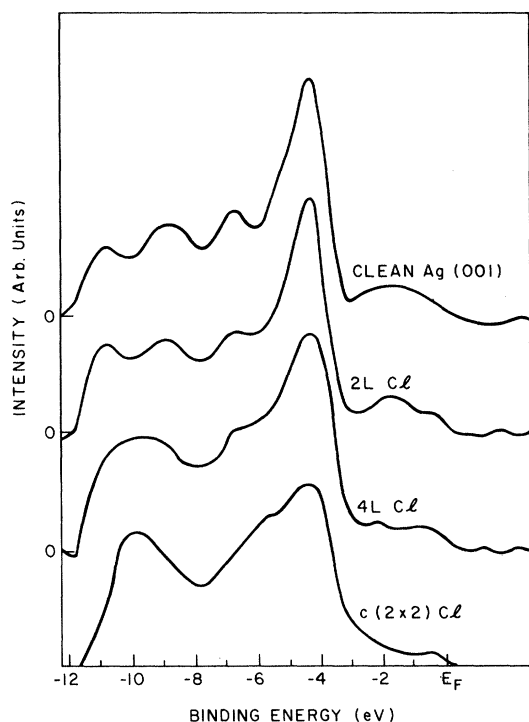


FIG. 2. Angle-integrated photoemission spectra for the clean Ag(001) surface, for several different exposures to chlorine gas, at photon energy of $\hbar\omega = 16.8$ eV. From Ref. 5.

mentum component parallel to the surface. The Cl feature at -3.5 eV has a relatively flat but slightly positive dispersion (at Γ) which would suggest a Cl $3p_z$ -like character for the wave function if the spectrum were interpreted as that of an isolated Cl layer. The lower, broader feature at -6 eV is found to have a negative dispersion at Γ and a width of about 0.75 eV which suggests considerable adatom-adatom interaction. The dispersion of the lower feature would suggest a Cl $3p_{x,y}$ character for the emitting bands in the isolated layer picture. Hybridized Ag orbitals may, of course, play a role in both features and obviate this interpretation.

In Fig. 4 we show the EDC's and calculated partial density of states (PDOS) for bulk AgCl.⁷ Since formation of a Cl adlayer is the first step toward bulk formation of AgCl, one might expect some similarity between the EDC's of the exposed surface and bulk compound. It is interesting to note that the p -symmetry PDOS of bulk AgCl shows a gap in the middle of the d band and reaches a maximum toward the top and bottom of the Ag d bands. The d -symmetry PDOS shows a peak in the middle of the d band and decreases to small values at the top and at the bottom of the d band. This behavior is qualitatively similar to the EDC's

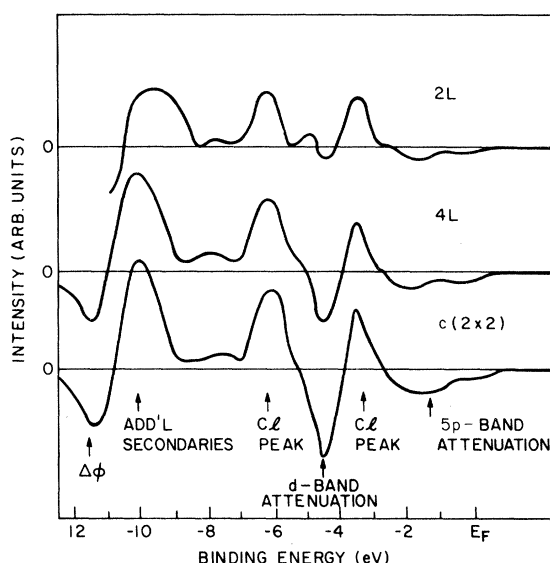


FIG. 3. Angle-integrated difference curves for several different exposures of the Ag(001) surface to chlorine. From Ref. 5.

in Figs. 2 and 3.

We may summarize the experimental data by observing that the LEED experiment favors the SOM, although the MLM gives agreement of roughly the same quality for many of the beam intensity profiles. The photoemission data shows two Cl-derived peaks at the top and at the bottom of the Ag d -band emission intensity. The dispersion of these peaks, obtained from ARUPS data, suggests considerable adatom-adatom interactions. Finally, the EDC's from bulk AgCl are roughly similar to those seen for the Cl-exposed surface and suggest that the chemical environments of the Cl atoms for the two cases are similar.

III. THEORETICAL METHODS

In the following we briefly review the essential details of our calculation. The reader is directed to Ref. 8 for a more complete discussion. The self-consistent electronic structure is solved by the use of *two* Gaussian bases, one for the wave functions and one to represent the spatial variations of the charge density and self-consistent potential. This allows us to reduce the evaluation of the Hamiltonian matrix to a manageable number of three-center integrals which can be evaluated analytically or, in the case of the local exchange-correlation potential, numerically on some grid of points in the unit cell.

The potential $V(\vec{x})$ describing the interaction of the electrons and nuclei may be expressed as a function only of the electron density $\rho(\vec{x})$ (which,

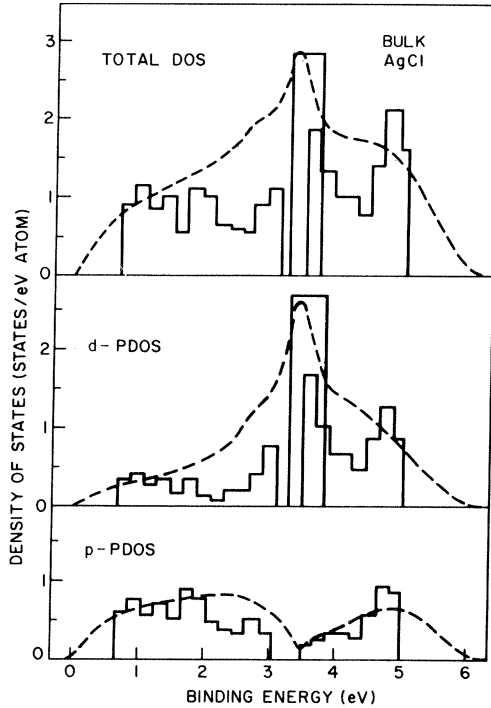


FIG. 4. Comparison of theoretical (---) and experimental (—) density of states for bulk AgCl (from Ref. 7). The two peaks in the p -symmetry DOS are roughly similar to the two Cl features in Fig. 3 and suggest some similarity to the chemical environments of the Cl atoms.

in turn, is the Brillouin-zone sum of the squares of all occupied wave functions evaluated at \vec{x} :

$$V(\vec{x}) = \int \frac{\rho(\vec{x}') d\vec{x}'}{|\vec{x} - \vec{x}'|} - \sum_{ij} \frac{Z_i}{|\vec{x} - \vec{R}_j - \vec{A}_i|} + V_{xc}(\rho(\vec{x})). \quad (1)$$

The first two terms are the electrostatic contribution from the electrons and nuclei, respectively, and the last term is a local density approximation to the exchange and correlation potential. We use Wigner's interpolation formula for V_{xc} .³ The lattice points are located at vectors \vec{R}_j , and nuclei of charge Z_i are located at vectors \vec{A}_i in the unit cell.

Both the charge density and potential are expanded in the same Gaussian basis, which is fixed for each model:

$$\rho(\vec{x}) = \sum_{jkl} \rho_{kl} \exp(-\alpha_{kl} |\vec{x} - \vec{B}_l - \vec{R}_j|^2) \quad (2)$$

and

$$V(\vec{x}) = \sum_{jkl} v_{kl} \exp(-\alpha_{kl} |\vec{x} - \vec{B}_l - \vec{R}_j|^2) - \sum_{ij} Z_i \frac{\exp(-\gamma_i |\vec{x} - \vec{A}_i - \vec{R}_j|^2)}{|\vec{x} - \vec{A}_i - \vec{R}_j|}. \quad (3)$$

The vectors \vec{B}_l define the sites of the potential and charge basis (PCB). The \vec{B}_l include the set of \vec{A}_l 's, but additional sites are introduced to enable high-angular-momentum components of $\rho(\vec{r})$ about atomic sites to be more accurately represented while using only spherically symmetric Gaussians. The second term in Eq. (3) describes the nuclear Coulomb singularity and has a very short range ($\gamma_i > 100$).

Once we fix the decay constants α_{kl} and the sites of the PCB \vec{B}_l , we evaluate ρ_{kl} and v_{kl} by a series of linear variational problems. For example, to determine the v_{kl} , assuming the ρ_{kl} are known, we substitute Eq. (2) into (1) and vary v_{kl} to minimize the root-mean-square difference between Eqs. (3) and (1). A similar minimization is carried out for the charge density obtained from the wave functions and Eq. (2), with the important additional constraint that charge neutrality is exactly preserved.

The valence wave functions of the slab $\psi_{\vec{k}}(\vec{x})$, with two-dimensional Bloch vector \vec{k} parallel to the surface and with energy $\epsilon_{\vec{k}}$, are expanded in a different Gaussian basis. They may be written

$$\psi_{\vec{k}}(\vec{r}) = \sum_{jnlm} c_{jnlm}^{\vec{k}} \phi_{jnlm}^{\vec{k}}(\vec{r}), \quad (4)$$

where

$$\phi_{jnlm}^{\vec{k}}(\vec{r}) = \sum_i \exp(i\vec{k} \cdot \vec{R}_i) u_{jnlm}(\vec{r} - \vec{R}_i - \vec{A}_j). \quad (5)$$

The $\phi_{jnlm}^{\vec{k}}$ are Bloch functions based on Gaussian, localized orbitals u_{jnlm} (labeled as atomic wave functions). The sum over i in Eq. (5) runs over sites in the two-dimensional Bravais lattice, while the sum over j in Eq. (4) runs over the basis sites of the unit cell. These sites include not only the positions of the Ag and Cl nuclei but also, in the case of the SOM, a supplementary wave-function site in the vacuum consisting of one s and three p orbitals with intermediate decay constants. This provides extra variational flexibility for the electrons to spill out into the vacuum. The localized functions u_{jnlm} , each a linear combination of Gaussians times spherical harmonics, are obtained from self-consistent atom calculations for Ag and Cl (Ref. 8) and are fixed once and for all for all five calculations [bulk Ag, clean Ag(001), isolated $c(2 \times 2)$ Cl layer, the SOM, and the MLM]. Similar expressions are used to represent the Ag and Cl core orbitals. After orthogonalizing the valence states to the core states, the core states are frozen, allowing one to diagonalize the Hamiltonian matrix with respect to the valence states only.

There are two important criteria that ensure the adequacy of a PCB. One is that global charge

conservation be approximately maintained when the constraint of exact charge neutrality is removed. Our self-consistent calculations were considered adequate when the unconstrained charge agreed with the constrained charge within $10^{-4}e$. The second criterion is that the PCB properly allows the surface charge density to decrease to zero in the vacuum, without unphysical Gibbs oscillations caused by the use of a finite basis. After some experimentation, three PCB's were found for the clean Ag(001) surface, the SOM, and the MLM which gave acceptable self-consistent charge densities that decreased smoothly to zero in the vacuum and led to reasonable work functions.

The lattice constant of the three-layer Ag slab was chosen to be 4.078 Å, the value for bulk Ag.¹³ The SOM was made by putting the Cl adatoms 1.88 Å above the slab surface, giving an Ag-Cl bond length roughly equal to the sum of the ionic radii of Ag and Cl. The MLM was made by putting Cl adatoms and Ag adatoms 1.66 and 1.91 Å, respectively, above the slab surface. These are the most likely values indicated by the LEED data⁴ and represent relaxation of the Ag-adatom layer in toward the slab surface by 0.13 Å. The unit cells of the SOM and MLM thus have eight atoms (80 valence electrons) and ten atoms (102 valence electrons), respectively. A self-consistent calculation for an isolated two-dimensional array of Cl atoms located in the same positions as the $c(2 \times 2)$ Cl layer was also performed.

The PCB was constructed in the following manner. Besides sites located at the atomic nuclei, extra sites were used in the tetragonal and octahedral pockets of the slab and for three layers above the surface to provide adequate variational freedom for the charge density. A similar PCB was used for the clean surface and MLM. In both the SOM and MLM, the $c(2 \times 2)$ arrangement of adatoms on one side was staggered with respect to that of the other side to minimize splitting of surface states because of the proximity of the two surfaces. The SOM and MLM then had a D_{2d} symmetry about the center of the octahedral pockets in the slab.

In order to carry out all the calculations economically a contracted valence basis was used to represent the Ag atoms.⁹ First, a self-consistent calculation of the band structure of bulk Ag was made with a full valence basis of 18 orbitals (two 5s, 6s; six 5p, 6p; ten 4d, 5d). The band structure was verified to give good agreement with earlier calculations and experiment.¹⁰ The basis was then contracted by replacing the six *p* orbitals by three superpositions of 5*p* and 6*p* orbitals. Similarly the ten *d* orbitals

were replaced by five superpositions of 4*d* and 5*d* orbitals. (That this was possible at all followed from a careful examination of the orbital content of the self-consistent wave functions obtained from the band calculations. The 6*p* and 5*d* orbitals consistently had roughly the same relative weights, about 0.165 and -0.030, with respect to the 5*p* and 4*d* orbitals, at different points in the Brillouin zone.) This reduces the 18 orbitals of the full basis to 10 orbitals in the contracted basis. Another self-consistent calculation of the band structure was then carried out for bulk Ag with the contracted basis. The Fermi level and various energy-state differences at symmetry points were found to agree within 0.3 eV with the values obtained using the full basis. This agreement was sufficiently good to allow us to use the contracted Ag basis in the remaining calculations.

The fits to the charge and potential were done in such a way as to monitor a possible overcompleteness of the PCB and to correct such overcompleteness if it occurred. The variational equations of the least-squares fit require the solution of a linear matrix equation

$$A\vec{x} = \vec{b}, \quad (6)$$

where *A* is the self-overlap matrix of the PCB and *b* is the integral of each PCB component times the function to be fit. By obtaining the eigenvalues and eigenvectors of the real symmetric matrix *A*,

$$A\vec{u}_i = \epsilon_i \vec{u}_i, \quad (7)$$

Eq. (6) could be inverted,

$$\vec{x} = \sum_i \frac{1}{\epsilon_i} (\vec{b} \cdot \vec{u}_i) \vec{u}_i. \quad (8)$$

Overcompleteness from, e.g., an improper range of decay constants α_{kl} , occurs when the eigenvalues ϵ_i are too small to be meaningful, given the limits of roundoff error and lattice-sum convergence. The corresponding eigenvector \vec{u} then has components which rapidly oscillate in sign so that $\vec{b} \cdot \vec{u}_i$ in Eq. (8) is small. The overcompleteness of the basis can then be removed indirectly by allowing only terms with ϵ_i greater than some positive cutoff into the sum of Eq. (8). We found that few, if any, terms had to be eliminated by this method and hence that the various bases were well designed.

We conclude this section by discussing how the total and partial densities of states (TDOS and PDOS) were calculated. Once the self-consistent Hamiltonian and wave functions have been obtained, one knows, in principal, the overlap matrix,

TABLE I. Calculated and experimental work functions and the layer charge per unit cell for the clean surface, the SOM and the MLM.

	Clean surface	SOM	MLM
Calculated work function (eV)	3.8	6.3	2.7
Experimental work function (eV)	4.4 ^a	5.2 ^a	5.2 ^a
Cl adatom charge per atom		7.66e ^b	7.96e
Ag adatom charge per atom			10.53e
1st Ag layer charge per atom	10.98e	10.68e	10.77e
2nd Ag (central) layer charge per atom	11.05e	10.99e	10.98e

^a J. Rowe, private communication.

^b The charge of the supplementary-wave-function site is included in this number.

$$S_{jnlm, j'n'l'm'}^{\vec{k}} = \int d^3\vec{r} \phi_{jnlm}^{\vec{k}*} \phi_{j'n'l'm'}^{\vec{k}}, \quad (9)$$

and the wave-function coefficients $c_{jnlm}^{\vec{k}}$ of Eq. (4) for all points in the Brillouin zone and for all eigenvalues at these points. The PDOS, projected onto some group of orbitals labeled by α , is then given by

$$\rho_{\alpha}(E) = \sum_{\vec{k}} \sum_{b} \sum_{\nu \in \alpha} \delta(E - E_{\vec{k}b}) \text{Re}(c_{jnlm}^{\vec{k}*} S_{\nu\nu'} c_{\nu'b}^{\vec{k}}), \quad (10)$$

where the summations extend over all members $\nu (=jnlm)$ of the group α , over all members of the basis ν' , over all k points in the Brillouin zone \vec{k} , and over all bands b .¹¹ The TDOS is then obtained by summing the $\rho_{\alpha}(E)$ over all distinct sets α .

Typically, a non-self-consistent run based on the self-consistent potential of a given model would be made at 15 special k points¹² in the $\frac{1}{8}$ irreducible wedge of the two-dimensional Brillouin zone. The infinite sum over k points in (10) was then approximated by a finite sum over the special points. The contribution of all eigenvalues at each special k point was then sorted into energy bins of width ~ 0.15 eV. The resulting DOS as a function of energy was then smoothed by convolution with a Gaussian of a full width at half maximum of 0.3 eV to approximate the instrumental resolution of the photoemission experiments.

To summarize this section, two Gaussian bases were used to reduce the computational complexity of a self-consistent LCAO calculation with a local exchange-correlation potential. Criteria were determined (and tested) to establish the suitability of the wave-function basis and potential-charge basis. A contracted valence basis was used for the Ag atoms and carefully tested against a full valence basis. The method of calculating the TDOS and PDOS was explained.

IV. RESULTS AND DISCUSSION

The calculated and experimental work functions and the layer charge per unit cell for the clean surface, the SOM, and the MLM are summarized in Table I. (The layer charge was obtained by integrating the local density of states on all orbitals of that layer up to the Fermi level.) The work functions for the clean surface and that of the MLM are too small when compared to the experimental values, while that of the SOM is too large. In addition, the *change* in work function upon adsorbing Cl in the $c(2 \times 2)$ position, 2.5 and -1.1 eV for the SOM and the MLM, respectively, are much larger than the experimentally observed difference, and the latter is of the wrong sign.

The small work function for the clean surface is probably due to our use of a three-layer slab to approximate the semi-infinite solid and, perhaps, to incomplete convergence of the PCB. Experience with this method has shown that work-function errors from an insufficiently converged charge fit have very little effect on the calculated spectrum referenced to the Fermi level.¹ The more extreme values of the work function for the SOM and the MLM most likely derive from the incorrect positioning of the Cl adatoms: too far out for the SOM and too close to the surface for the MLM. The Cl layer charge per unit cell shows considerable electron transfer—over half an electron—to the Cl adatoms in both models. This creates a sizable surface dipole which is quite sensitive, due to the requirement of self-consistency, to the distance of the Cl adatoms to the surface.¹⁴ The change in work function is consistent with creating a large negative planar charge just outside the surface for the SOM and just inside the surface for the MLM. The experimental surface evidently lies between these extremes.

The Cl atom in the MLM has picked up an entire electron so that the MLM, although the surface

Ag atoms are not fully ionized, is quite similar to bulk AgCl. The central Ag layer of the slab remains neutral in all three cases and suggests that a three-layer slab, while too thin to give a well converged band structure, is thick enough to screen perturbations in the surface charge distribution.

This last point may be seen more clearly if we turn to the calculated PDOS's of the three models (Fig. 5, 6, and 7). The PDOS's of the first Ag layer in the SOM and MLM (Figs. 6 and 7) show features due to the interaction with the Cl adatoms which disappear by the time one has reached the central layer. The central layer PDOS is similar to that, in turn, of the clean Ag(001) surface. This suggests that the strong perturbations from the Cl adatoms are fully screened at the central layer. This strong, local screening and "healing" of surface charge perturbations is a general feature of metal surfaces.¹⁵

If we compare the TDOS of the three models with the photoemission EDC's in Figs. 2 and 3, we see that the MLM has two Cl features that correspond to the data, while the SOM has a two-peaked Cl feature only on the upper part of the Ag *d* bands. Here it is important to look at the LDOS on the Cl orbitals of the SOM [Fig. 6(b)].

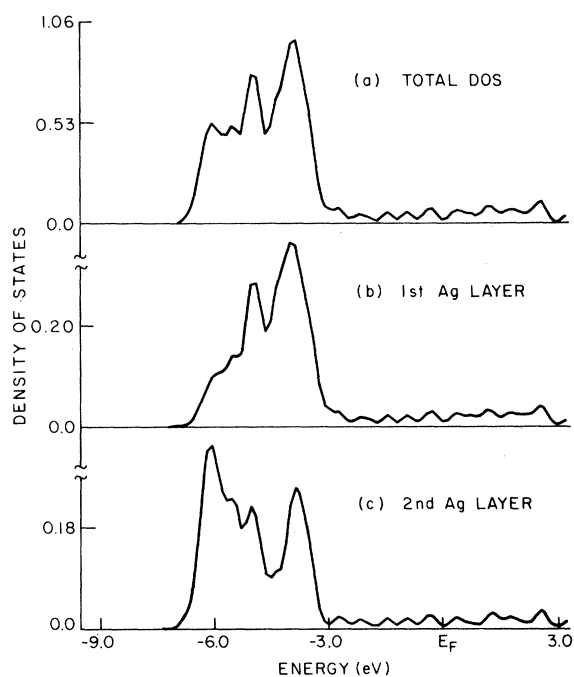


FIG. 5. TDOS and PDOS calculated for the clean Ag(001) surface. (a) The TDOS. (b) The PDOS of the first Ag layer. (c) The PDOS of the central (second) Ag layer. The vertical scale in this figure and in Figs. 6, 7, and 8 is measured in units of 7.85 states/eV.

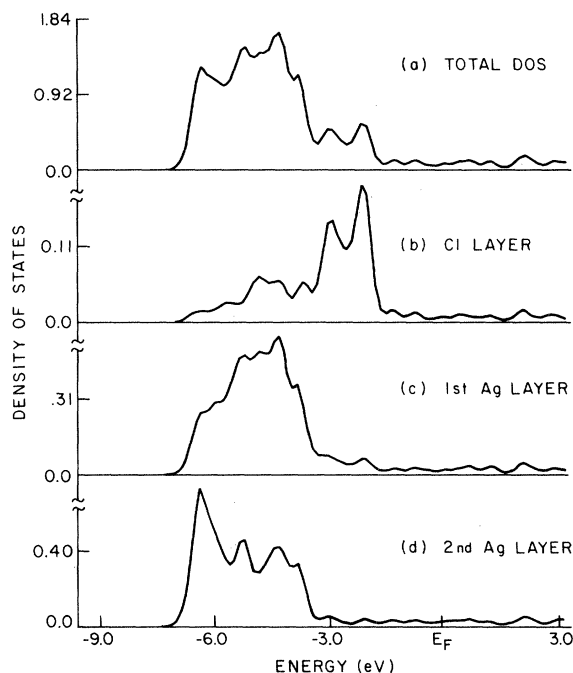


FIG. 6. TDOS and PDOS calculated for the SOM. (a) The TDOS. The two-peaked, Cl-derived feature lies above the Ag *d* bands. (b) The Cl PDOS. There is no significant weight toward the bottom of the Ag *d* bands, contrary to the photoemission data. (c) The PDOS of the first Ag layer. (d) The PDOS of the central (second) Ag layer.

There is no weight towards the bottom of the Ag *d* bands so that a Cl feature is not "hiding" in the SOM TDOS in that region. It is interesting to note, however, that Cl-induced structure of this sort has been observed on the Ag(110) surface.¹⁶ An overlayer model has been proposed for this surface,¹⁷ and while the geometry is different in detail from that considered here, our results lend at least some support to that proposal.

If we project the DOS onto the Cl $3p_x$, $3p_y$, $3p_z$ orbitals, respectively, for the SOM and MLM (not shown), we find that all three PDOS are roughly the same and similar to those in Figs. 6(b) and 7(b), provided the figures are scaled by $\frac{1}{3}$. The three Cl *p* orbitals contribute equally to the bonding and none of the Cl features in the SOM or in the MLM are due to Cl *p* orbitals of a particular symmetry. Examining the Cl induced states near the zone center for the SOM, we do indeed find that the p_z -like states disperse up and the p_x, p_y -like states disperse down. However, this has nothing to do with the dispersion measured in ARUPS,⁶ since both these states lie in the peak above the *d* band. The Cl *p* orbitals primarily have indirect interactions through the coplanar Ag's in the MLM, and the simple rules for identifying

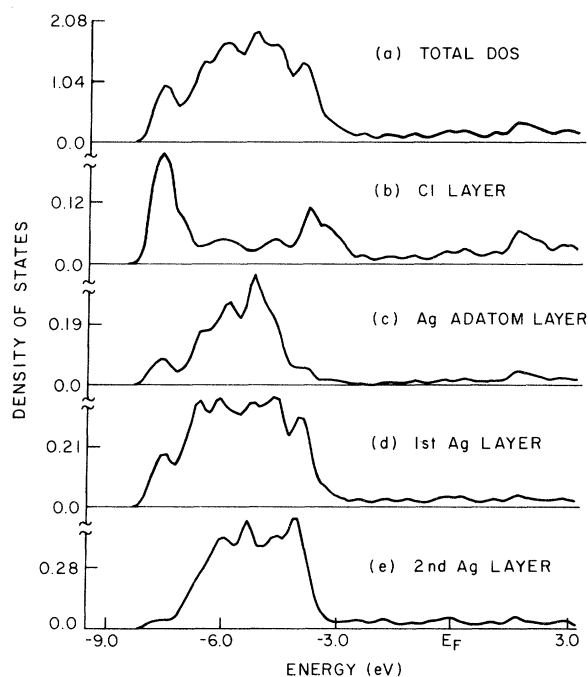


FIG. 7. TDOS and PDOS calculated for the MLM. (a) The TDOS. There is now a Cl feature on either side of the Ag d bands, in accordance with the photoemission data. (b) The Cl PDOS. (c) The PDOS of the Ag adatom, which is roughly coplanar with the Cl adatom. (d) The PDOS of the first Ag layer. (e) The PDOS of the central (second) Ag layer.

dispersion with orbital symmetry are invalid. For example, a low-lying state occurs which includes hybridized Cl p_x and Ag d_{xz} orbitals, and this disperses upward at Γ . Thus the apparent disagreement between the orbital content of the Cl features found here and that inferred in Ref. 6 is resolved.

The extent to which adatom-adatom interactions play a role may be determined by comparing the TDOS of an isolated, two-dimensional Cl layer in the $c(2 \times 2)$ arrangement with the PDOS projected onto the Cl orbitals of the SOM (Fig. 8). The width of the TDOS of the isolated Cl layer gives the dispersion of the Cl bands from direct Cl-Cl interactions, here about 0.5 eV. The extra broadening (0.25 eV) seen in the SOM Cl PDOS presumably comes from the indirect interactions of the Cl adatom through the Ag d bands. Surprisingly, most of the dispersion in the SOM comes from direct interactions although the Cl adatoms are about 4 Å apart on the surface. The strong interactions between the Ag and Cl atoms in the MLM, which split states off from the bottom of the d band, produce hybridized states for which the direct-indirect distinction is not meaningful.

V. SUMMARY AND CONCLUSION

The apparent disagreement of the geometries selected by LEED analysis⁴ and by the combinations of ARUPS (Ref. 5) and the present electronic structure analysis is disturbing. The case of N chemisorbed on Ti(0001) was studied by a LEED analysis¹⁸ completely paralleling that for Cl on Ag,⁴ and an electronic structure calculation using methods identical to those employed here.¹⁹ Satisfactory agreement with ARUPS was obtained for the LEED-selected underlayer model, and alternative overlayer models could be convincingly ruled out.¹⁹

For the present system it is certainly physically plausible to anticipate a mixed-layer geometry with coplanar or nearly coplanar Cl and Ag.^{4,17} A coplanar $c(2 \times 2)$ layer is nearly identical to a (001) plane of an AgCl crystal. The nearest-neighbor bond length is just 0.1 Å greater for the mixed layer than for the compound, indicating that the energetics are nearly optimized by such an arrangement. This near epitaxy, combined with a comparison of the surface spectrum⁶ with the bulk AgCl photoemission discussed previously,⁷ would have prompted one to guess this geometry even in the absence of the present calculations. It would not, of course, be clear to

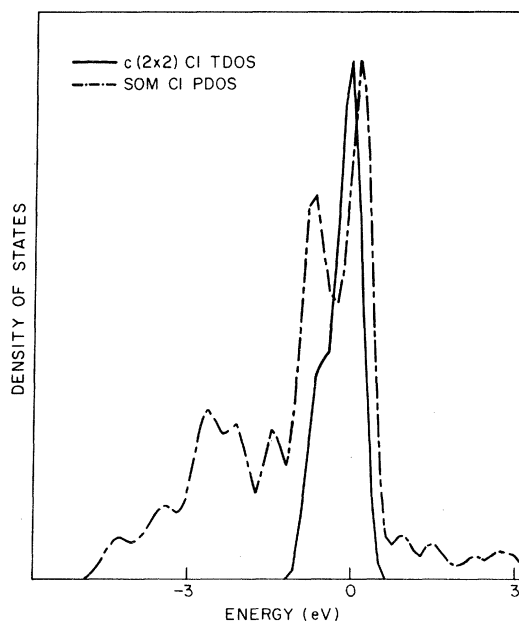


FIG. 8. The Cl PDOS of the SOM (---) compared with the calculated TDOS of the isolated $c(2 \times 2)$ Cl lattice (—). The width of the TDOS of the isolated Cl layer gives the dispersion due to direct Cl-Cl interaction. The extra broadening of the Cl PDOS of the SOM is due to indirect interactions mediated by substrate Ag d orbitals.

what extent the overlayer model might have a similar spectrum.

The mixed-layer geometry with the Cl layer slightly inside the Ag layer was used because it corresponded to the best LEED fit for this model. The work-function decrease found in our calculations is consistent with a net dipole decrease accompanying the large Ag-to-Cl charge transfer. The experiment indicates a 0.8-eV work-function increase, which would suggest raising the Cl above the Ag in the mixed layer. This might be expected on the basis of size considerations. The mixed layer is quite strongly ionized. Ag⁺ and Cl⁻ have ionic radii of 1.26 and 1.81 Å, respectively, and both must fit against similar sites on the first substrate layer. Such small adjustments in geometry would not be expected to produce a significant change in the mixed-layer spectrum.

The overlayer model shows a work-function increase much larger than experiment. The overlayer-model calculation was performed using the AgCl bond length. This is within the quoted uncertainty of the LEED fit, but puts the Cl layer 0.16 Å further above the surface than the optimum LEED choice. Decreasing the distance should decrease the excess dipole somewhat, but the spectrum could not be reasonably expected to show the qualitative changes needed to make this model agree with the photoemission results. As noted previously, the overlayer spectrum is in qualitative agreement with experiment for Cl on

Ag(110). The increase in work function upon adsorption observed in this case is 1.7 eV, significantly greater than for (100), which is consistent with the expected difference in dipole between mixed and overlayer models.¹⁷

The possibility must be considered that the LEED experiment was done on a different surface than the ARUPS experiment. The surface used in the LEED studies was prepared by exposing a clean Ag(001) surface to dichloroethane (C₂H₄Cl₂) at 100 mTorr pressure and at 150 °C for several minutes.⁴ The surface prepared for the ARUPS experiment was obtained by exposing a clean Ag(001) surface to pure chlorine gas at pressures below 5 × 10⁻⁴ mTorr and at room temperature.⁵ Just possibly these different methods lead to different c(2 × 2) configurations of Cl on the Ag surface. The temperatures used in both preparations are sufficiently high, however, that one might expect the surface atoms to equilibrate (recalling the high ionic mobility generally shown by Ag halides). Nonetheless, it is necessary that LEED intensity measurements and UPS measurements be done *in situ* on the same surface before definite conclusions are drawn.

ACKNOWLEDGMENTS

We thank P. J. Feibelman, F. Jona, and J. E. Rowe for helpful discussions. One of the authors (H.S.G.) gratefully acknowledges financial support from the National Science Foundation.

¹P. J. Feibelman and D. R. Hamann, *Phys. Rev. B* **21**, 1385 (1980); S. G. Louie, *Phys. Rev. Lett.* **42**, 476 (1978).

²B. Lundquist, H. Hjelmberg, and O. Gunnarsson, *Photoemission and Electronic Properties of Solids*, edited by B. Feuerbacher, B. Fitton, and R. F. Willis (Wiley, London, 1978).

³E. Wigner, *Phys. Rev.* **46**, 1002 (1934).

⁴E. Zanazzi, F. Jona, D. W. Jepsen, and P. M. Marcus, *Phys. Rev. B* **14**, 432 (1976).

⁵S. P. Weeks and J. E. Rowe, *J. Vac. Sci. Technol.* **16**, 470 (1979).

⁶S. P. Weeks and J. E. Rowe, *Solid State Commun.* **27**, 885 (1978).

⁷J. Tejeda, N. J. Shevchik, W. Braun, A. Goldmann, and M. Cardona, *Phys. Rev. B* **12**, 1557 (1975).

⁸P. J. Feibelman, J. A. Appelbaum, and D. R. Hamann, *Phys. Rev. B* **20**, 1433 (1979).

⁹A full set of 13 valence orbitals (3s, 4s, 3p, 4p, 3d) was retained for the Cl atom basis since at most two Cl atoms occur per unit cell.

¹⁰E. C. Snow, *Phys. Rev.* **172**, 708 (1968). This calculation used an $\alpha = 1$ and $\alpha = \frac{5}{8}$ Slater term for the ex-

change and correlation potential and gave agreement with our values only when the various energy-state differences were linearly extrapolated to $\alpha = \frac{2}{3}$, which approximates the Wigner potential.

¹¹D. G. Dempsey and L. Kleinman, *Phys. Rev. B* **16**, 5356 (1977).

¹²A. Baldereschi, *Phys. Rev. B* **7**, 5212 (1973); D. J. Chadi and M. L. Cohen, *ibid.* **8**, 5747 (1973); M. J. Monkhorst and J. D. Pack, *Phys. Rev.* **13**, 5188 (1976).

¹³R. W. G. Wyckoff, *Crystal Structures*, 2nd ed. (Interscience, New York, 1963).

¹⁴If one smears the observed Cl layer charge onto two planes of opposite charge, separated by 1.9 Å as in the SOM, the potential difference is ~10 eV, the right order of magnitude.

¹⁵P. J. Feibleman, *J. Vac. Sci. Technol.* **17**, 176 (1980).

¹⁶D. Briggs, R. A. Marbrow, and R. M. Lambert, *Chem. Phys. Lett.* **53**, 462 (1978).

¹⁷G. Rovida and F. Pratesi, *Surf. Sci.* **51**, 270 (1975).

¹⁸H. D. Shih, F. Jona, D. W. Jepsen, and P. M. Marcus, *Surf. Sci.* **60**, 445 (1976).

¹⁹P. J. Feibelman and F. J. Himpsel, *Phys. Rev. B* **21**, 1394 (1980).